

# Preparation of Ag, Pd, and Pt<sub>50</sub>-Ru<sub>50</sub> colloids prepared by $\gamma$ -irradiation and electron beam and electrochemical immobilization on gold surface

Kyung-Hee Kim<sup>1</sup>, Kang-Deuk Seo<sup>1</sup>, Seong-Dae Oh<sup>1</sup>, Seong-Ho Choi<sup>1\*</sup>,  
Sang-Hyub Oh<sup>2</sup>, Jin-Chun Woo<sup>2</sup>, A. Gopalan<sup>3</sup> and Kwang-Pill Lee<sup>3</sup>

<sup>1</sup>Department of Chemistry, Hannam University, 133 Ojung-Dong, Daeduck-Gu, Daejeon 306-791, South Korea

<sup>2</sup>Div. of Chemical Metrology and Materials, Evaluation/Organic Analysis Group, Korea Research

Institute of Standard and Science, Daejeon 305-600, South Korea

<sup>3</sup>Department of Chemistry Graduate School, Kyungpook National University,

Daegu 702-701, South Korea

(Received July 24, 2006; Accepted August 3, 2006)

**Abstract :** PVP-protected Ag, Pd and Pt<sub>50</sub>-Ru<sub>50</sub> colloids were prepared independently by using  $\gamma$ -irradiation and electron beam (EB) at ambient temperature. UV-visible spectra of these colloids show the characteristic bands of surface resonance and give evidence for the formation of nanoparticles. Transmission electron microscopy (TEM) experiments were used to know the morphology of nanoparticles prepared by  $\gamma$ -irradiation and EB. The size of Ag, Pd, and Pt<sub>50</sub>-Ru<sub>50</sub> nanoparticles prepared by  $\gamma$ -irradiation was *ca.* 13, 2-3, 15 nm, respectively. While, the size of Ag, Pd, and Pt<sub>50</sub>-Ru<sub>50</sub> nanoparticles prepared by EB was *ca.* 10, 6, and 1-3 nm, respectively. Cyclic voltammograms (CV) were recorded for the Au electrodes immobilized with these nanoparticles. CVs indicated the modifications in the surface as a result of immobilization.

**Key words :**  $\gamma$ -Irradiation/Electron beam/Ag colloids/Pd colloids/Pt<sub>50</sub>-Ru<sub>50</sub> colloids/Cyclic voltammetry

## 1. Introduction

Metal nanoparticles have attracted considerable attention recently because of their interesting physical/chemical properties and their potential applications.<sup>1-8</sup> Nanoparticles consist of several tens or hundreds of metal atoms. As a result of reduction in particle size and number of metal atoms, nanoparticle shows quantum size effect and other interesting properties. The size limitation introduces high population of atoms on the surface. Some of the most important properties are: the lower effective Debye

temperature,<sup>9</sup> the increased solid-solid transition pressure,<sup>10</sup> the higher self diffusion coefficient,<sup>11</sup> the higher thermal diffusivity,<sup>12</sup> and a variety of optical dispersion and nonlinear effects.<sup>13</sup> It is also attracting the possibility to control the properties of these materials by changing their shape, size and distribution.<sup>14</sup> Hence, it is very important to have the possibility to develop and optimize preparation techniques that can control these parameters. Varieties of media have been tried in order to both control the nanoparticle sizes and to offer stabilizing effect avoiding aggregation phenomenon.

\* Corresponding author

Phone : +82-(0)42-629-7467 Fax : +82+(0)42-629-7469

E-mail: shchoi@hannam.ac.kr

Nanoparticles have been prepared by chemical and physical methods giving the possibilities to control the microstructures. Few studies have been focused on the preparation of metal nanoparticles using UV and  $\gamma$ -irradiation.<sup>15,16</sup> We have reported the preparation of Ag nanoparticles in aqueous solution by using  $\gamma$ -irradiation.<sup>6,7</sup>

Electron beam irradiation can reduce noble metal ions to prepare metal nanoparticles. This can also be considered as a simple and clean reducing. These methods have many advantages for preparation of metal nanoparticles. For example, they are no reducing reagents, and a large number of metal nuclei are produced homogeneously and instantly. However, a little has been reported the preparation of the metallic colloids by using electron beam.

Water-soluble homopolymers such as poly(N-vinyl-2-pyrrolidone) (PVP) have been widely used as protective matrix for noble metal colloids in organic solvents.<sup>17</sup> The nano-scale colloidal metal particles protected by polymers not only exhibit intriguing properties due to their size effect but also provide the additional option of influencing the properties. Recently, well dispersed Prussian blue nanoparticles protected by PVP have been prepared by mixing aqueous  $\text{Fe}^{2+}$ ,  $[\text{Fe}(\text{CN})_6]^{3-}$ , and PVP solutions together.<sup>18</sup> It is noteworthy that the PVP-protected those nanoparticles show an increased solubility in a variety of organic solvents.

In this study, PVP-protected Ag, Pd and Pt-Ru nanoparticles were prepared by using  $\gamma$ -irradiation and EB in aqueous solution at ambient temperature. The obtained nanoparticles were analyzed by using UV-visible spectroscopy, transmittance electron microscopy (TEM) to compare physical properties of nanoparticles. Furthermore, the electrochemical properties of precious metallic nanoparticles were examined by using cyclic voltammetry.

## 2. Experimental

### 2.1. Materials

$\text{H}_2\text{PtCl}_6 \cdot x\text{H}_2\text{O}$  (37.5% Pt),  $\text{RuCl}_3 \cdot x\text{H}_2\text{O}$  (41.0% Ru), and  $\text{PdNO}_3$  were analytical reagent grade and supplied

by Aldrich-Sigma Co.  $\text{AgNO}_3$  was purchased from Kojima Chemicals Co., Ltd. (Japan). PVP (MW. av. 10,000) was obtained from Tokyo Kasei (Japan). Other chemicals of reagent grade were also used.

### 2.2. Preparation of PVP-stabilized Ag, Pd and Pt-Ru colloids by $\gamma$ -irradiation and electron beam

Ag colloids ( $9.0 \times 10^{-3}$  M of the precursor) were prepared as follows: A mixture solution was prepared having  $\text{AgNO}_3$  (0.31 g), 2-propanol (12 mL) as a radical scavenger, and PVP (2.0 g) as a colloidal stabilizer in distilled water (188 mL). Nitrogen gas was purged for 30 min. to remove the dissolved oxygen. The mixture solution was then irradiated by Co-60  $\gamma$ -ray source or electron beam.

Pd colloids ( $9.0 \times 10^{-4}$  M of the precursor) were prepared in a similar procedure to the Ag colloids. The mixture solution contained  $\text{PdNO}_3$  (0.04 g), 2-propanol (12 mL) as a radical scavenger, and PVP (2.0 g) as a colloidal stabilizer in distilled water (188 mL) in this case.

PVP-protected  $\text{Pt}_{50}\text{-Ru}_{50}$  alloy colloids were prepared by keeping  $\text{H}_2\text{PtCl}_6 \cdot x\text{H}_2\text{O}$  (0.02 g) and  $\text{RuCl}_3 \cdot x\text{H}_2\text{O}$  (0.02 g) in the solution prepared by dissolving 2.0 g of PVP in 188 mL of deionized water. On irradiation, dark brown-colored colloidal dispersions of precious metals were obtained.

### 2.3. Measurements

Absorption spectra of the PVP-stabilized Ag, Pd, and  $\text{Pt}_{50}\text{-Ru}_{50}$  colloids were recorded with UV-240 Shimadzu UV-VIS spectrophotometer using quartz cells. Transmission Electron Microscopy photographs of the samples were recorded using Energy Filtered Transmission Electron Microscope (EF-TEM, EM 912 Omega, Carl Zeiss, Germany) installed at Korea Basic Science Institute, Korea.

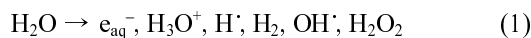
Cyclic voltammogram (CV) of the colloids were recorded using a 283 Potentiostat/Galvanostat (Princeton Applied Research, France). Platinum wire was used as a outer electrode. Silver/silver chloride and gold foil were used as reference as working electrodes, respectively. 0.5M  $\text{H}_2\text{SO}_4$  was

used as the electrolyte. A scan rate of 50 mV/sec was used. Electrochemical measurements were recorded after expulsion of dissolved oxygen from the colloidal solutions.

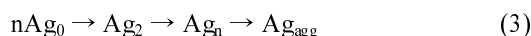
### 3. Results and Discussion

High energy irradiations like  $\gamma$ -irradiation can reduce the metal ions through generation of active species from the solvent or any other additive substances. This approach has been used for the preparation of few of the variety of metal nanoparticles.<sup>15,16,19</sup> In our experimental approach, the use of  $\gamma$ -irradiation or EB can effectively produce such active species, hydrated electron from water that was used as the medium.

Briefly, the mechanism of formation of Ag nanoparticles using  $\gamma$ -irradiation or EB is given here. In aqueous solution, hydrated electrons could be generated during  $\gamma$ -irradiation (Equation 1).



Reduction of silver ions with hydrated electrons could result formation of Ag colloids:



where n is the number of the aggregation of a few units and Ag<sub>agg</sub> is the aggregate in the final stable state. Likewise, Pd and Pt<sub>50</sub>-Ru<sub>50</sub> nanoparticles col-

loids were formed by employing  $\gamma$ -radiation or EB.

Fig. 1 shows the TEM images and absorption spectra of PVP-protected Ag colloids prepared by employing  $\gamma$ -irradiation at room temperature. Spherical-type Ag particles of the size of 13 nm were formed with a narrow size distribution in aqueous solution at room temperature. Concurrently, UV-visible spectrum of Ag colloids have characteristic surface plasmon peak at 407 nm due to particles size.<sup>20-22</sup> The presence of silver (0) in solution is represented by a broad and strong absorbance peak whose maximum occurs around 410 nm. The optical absorption and scattering of metal particles are due to the excitation of surface plasmons of small metal particles by an external oscillating electric field. When the particle size is small enough compared with the wavelength of light, their optical spectra are predominantly attributed to light absorption by dipole polarization of particles.<sup>23</sup> For bulk metals these resonant wavelengths are usually located in the IR portion of the spectrum. For the nanoparticles, the gap between the excitation bands is widened. A widened gap will absorb a photon of a higher energy level (visible spectrum). It is important to note that before solution before exposing did not show this characteristic peak (Fig. 1). Characterization of Ag colloids prepared by  $\gamma$ -irradiation are in accordance with earlier reports.<sup>5-7,16</sup>

Fig. 2 shows the TEM image and absorption spectrum of Pd nanoparticles prepared by  $\gamma$ -irradiation. PVP-protected Pd nanoparticles were found to be

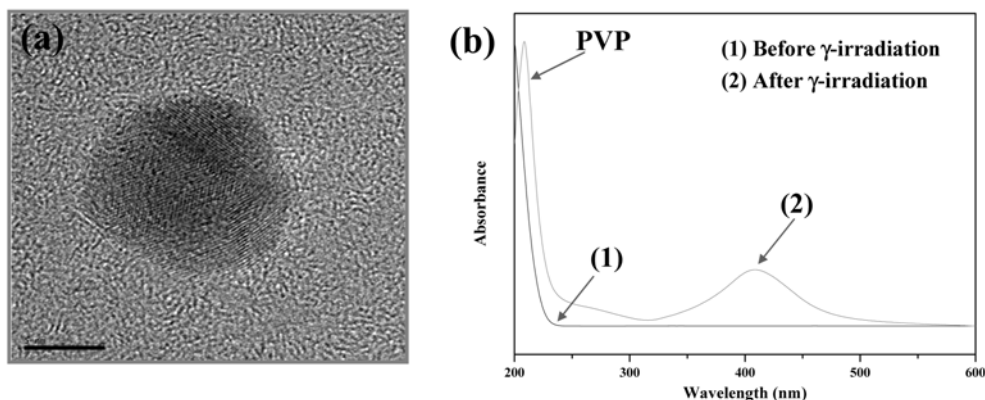


Fig. 1. TEM image (a) and UV-VIS spectra (b) of PVP-protected Ag nanoparticles prepared by  $\gamma$ -irradiation.

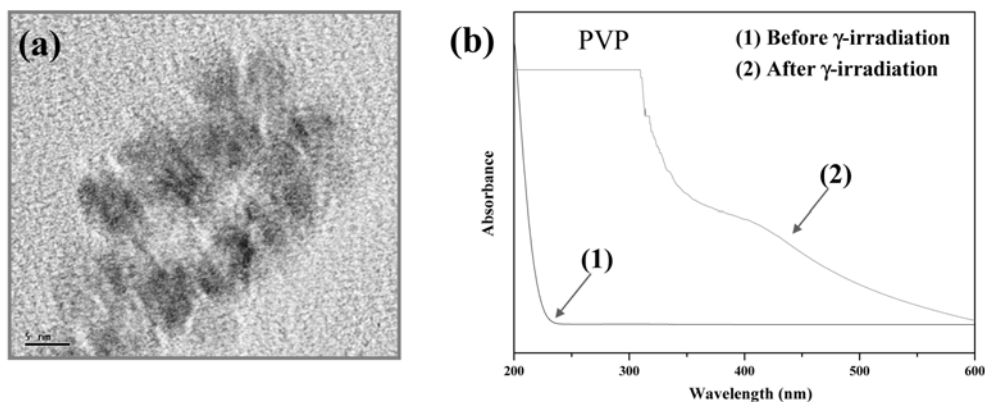


Fig. 2. TEM image (a) and UV-VIS spectra (b) of PVP-protected Pd nanoparticles prepared by  $\gamma$ -irradiation.

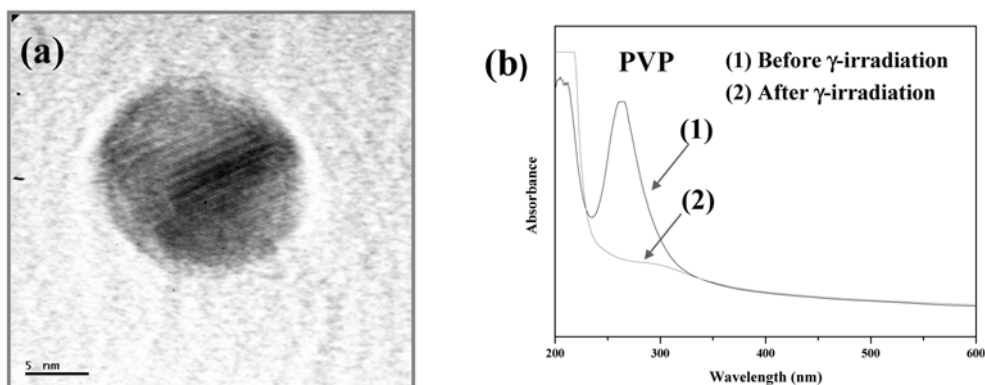


Fig. 3. TEM image (a) and UV-VIS spectra (b) of PVP-protected Pt<sub>50</sub>-Ru<sub>50</sub> alloy nanoparticles prepared  $\gamma$ -irradiation.

amorphous-type nanoparticles (Fig. 2). Smaller nanoparticles were found to be aggregated into secondary particles. Sizes of the Pd nanoparticles were estimated in the range of 2-3 nm. Absorption spectrum of Pd colloids (Fig. 2) showed the weak surface plasmon peak around 400 nm.<sup>24,25</sup> An increase in the intensity at the shorter wavelengths (nm) was taken as due to the broad distribution of nanoparticles size.<sup>26</sup>

Fig. 3 shows TEM images and absorption spectrum of the PVP-stabilized Pt<sub>50</sub>-Ru<sub>50</sub> nanoparticles. A 50% weight ratio of metal ions-to-PVP was maintained. TEM pictures indicated that the nanoparticle was aggregated into secondary particles (Fig. 2). It is presumed that smaller nanoparticles formed at the initial stages of irradiation might be aggregated into secondary particles, at the later stages. A distinct decrease in the intensity of the absorption peak 260

nm was observed. The peak at 260 nm may be taken as due to the probable complexation between the metal ions and PVP. The obvious decrease in the intensity of peak that represents complexation indicated that nanoparticles were generated through the reduction of metal ions from the complexed state.

Use of EB irradiation also resulted nanoparticles colloids but with differences in size distributions. Fig. 4 shows the TEM images and absorption spectra of PVP-protected Ag colloids prepared by using EB. TEM picture informs that spherical-type Ag particles of the size of 10 nm were formed with a narrow size distribution were produced in aqueous solution at room temperature by simultaneously than noticed with  $\gamma$ -irradiation. The size of Ag nanoparticles was smaller with EB than by  $\gamma$ -irradiation (see, Fig. 1). Otherwise, EB permeates more than  $\gamma$ -irradiation and disperses the nanoparticles. UV-visible

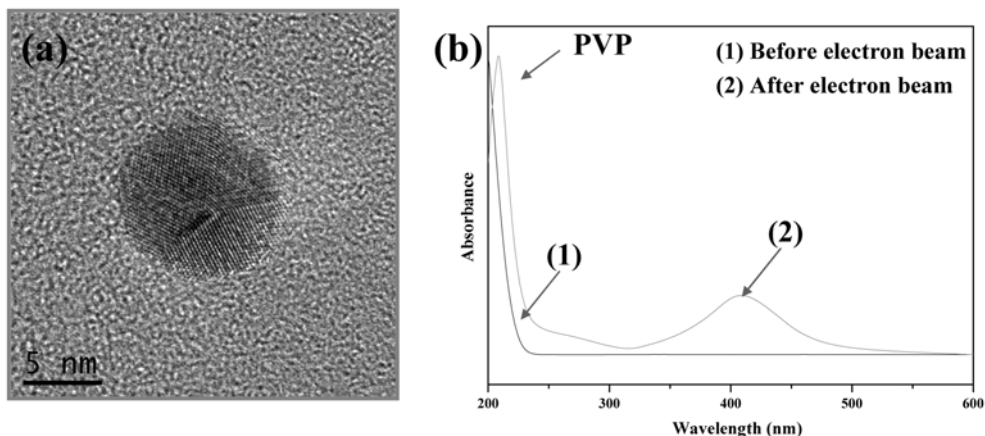


Fig. 4. TEM image (a) and UV-VIS spectra (b) of PVP-protected Ag nanoparticles prepared by electron beam.

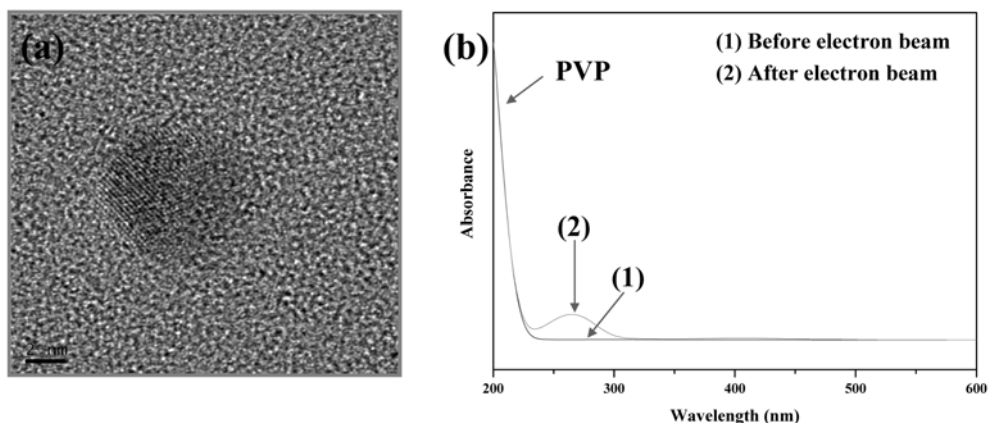


Fig. 5. TEM image (a) and UV-VIS spectra (b) of PVP-protected Pd nanoparticles prepared by electron beam.

spectrum of the of Ag colloids showed the surface plasmon peak<sup>20-22</sup> at 407 nm (Fig. 4) as noticed similar with  $\gamma$ -irradiation (Fig. 1).

Fig. 5 shows the TEM images and absorption spectra of Pd nanoparticles prepared by EB. Spherical-type nanoparticles with an average size of 6 nm were formed (Fig. 5). The existence of weak surface plasmon peak at 260 nm indicated a narrow distribution of nanoparticles sizes.<sup>26</sup>

Pt-Ru catalysts prepared by chemical reduction were proved to be highly active catalysts for the direct methanol fuel cell.<sup>27-29</sup> We are reporting here the preparation of Pt-Ru alloy nanoparticles colloids by using EB. It is pertinent to note that we have not used any additional reducing agents that are

expected to lower the efficiency of Pt-Ru catalysts through poisoning with the side products.

Fig. 6 shows TEM images and absorption spectra of the PVP-stabilized Pt<sub>50</sub>-Ru<sub>50</sub> nanoparticles prepared by EB. The size of Pt<sub>50</sub>-Ru<sub>50</sub> nanoparticles were in the range of 1-3 nm (Fig. 6). The features of the absorption spectrum of Pt<sub>50</sub>-Ru<sub>50</sub> colloids prepared by EB are similar to colloids prepared by  $\gamma$ -irradiation.

Electrochemical behavior of precious metallic nanoparticles on the Au electrode surface was monitored through cyclic voltammetry. Cyclic voltammograms (CVs) were collected at room temperature by configuring a micro-cell with a three-electrode assembly in 0.5M H<sub>2</sub>SO<sub>4</sub> and cycling the potential between

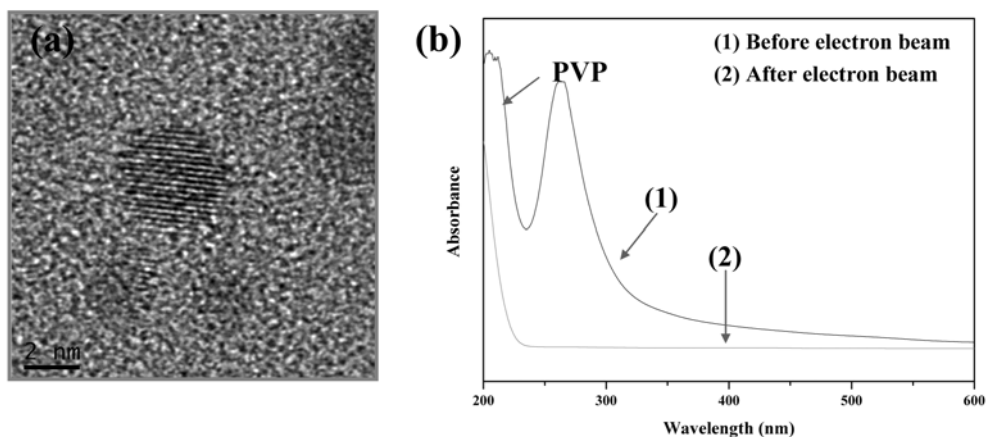


Fig. 6. TEM image (a) and UV-VIS spectra (b) of PVP-protected Pt<sub>50</sub>-Ru<sub>50</sub> nanoparticles prepared by electron beam.

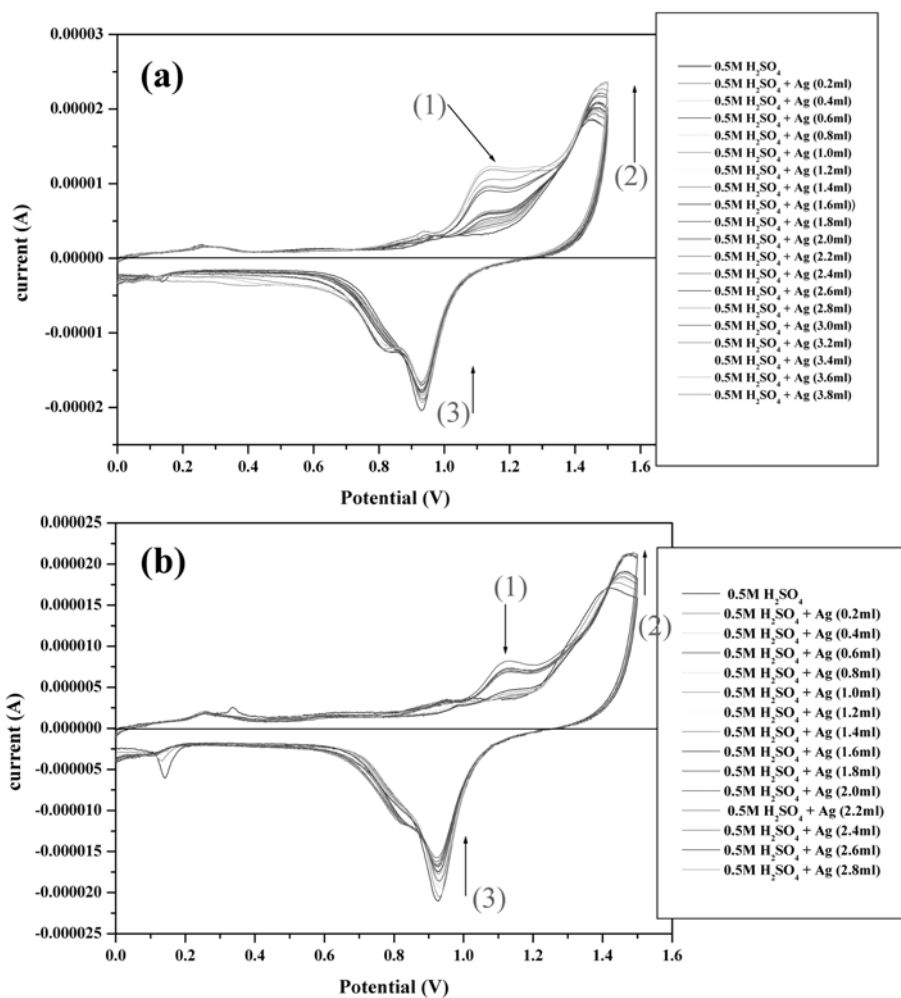


Fig. 7. CV curves of Au electrode in 0.5M H<sub>2</sub>SO<sub>4</sub> with Ag nanoparticles prepared by  $\gamma$ -irradiation (a) and prepared by e-beam (b).

0 and +1.5V (vs. Ag | AgCl). *s* 7 shows the CVs of Au electrode in 0.5M H<sub>2</sub>SO<sub>4</sub> with a sequential addition of Ag nanoparticles colloids prepared by  $\gamma$ -irradiation (a) and (b) prepared by EB. CVs were analyzed by the integration of the cathodic peak, (2) and (3) that represent the formation of superficial AuO and indicative of the surface area of the Au electrode (Fig. 7).<sup>30,31</sup> The modifications in the surface area of the Au electrode as a result of occlusion of Ag colloids can be witnessed from the new peak, (1), due to immobilization of Ag nanoparticles onto Au surface. The pattern of CV curves for the Ag colloids loaded Au electrodes, recorded with Ag col-

loids prepared by  $\gamma$ -radiation (Fig. 7a), were apparently similar to the CVs recorded with the Ag colloids prepared by EB (Fig. 7b). However, there are subtle differences in the surface areas, probably due to the differences in the size of the nanoparticles.

CVs of Au electrode recorded with the different loading of Pd nanoparticles prepared by  $\gamma$ -irradiation (a) and prepared by e-beam (b) are presented (Fig. 8). The peak at 1.1 V represents the immobilization of nanoparticles while using Pd nanoparticles prepared by  $\gamma$ -irradiation Fig. 8 (a). On the contrary, when Pd nanoparticles prepared by EB was used for modifying the Au electrode, the immobilization of

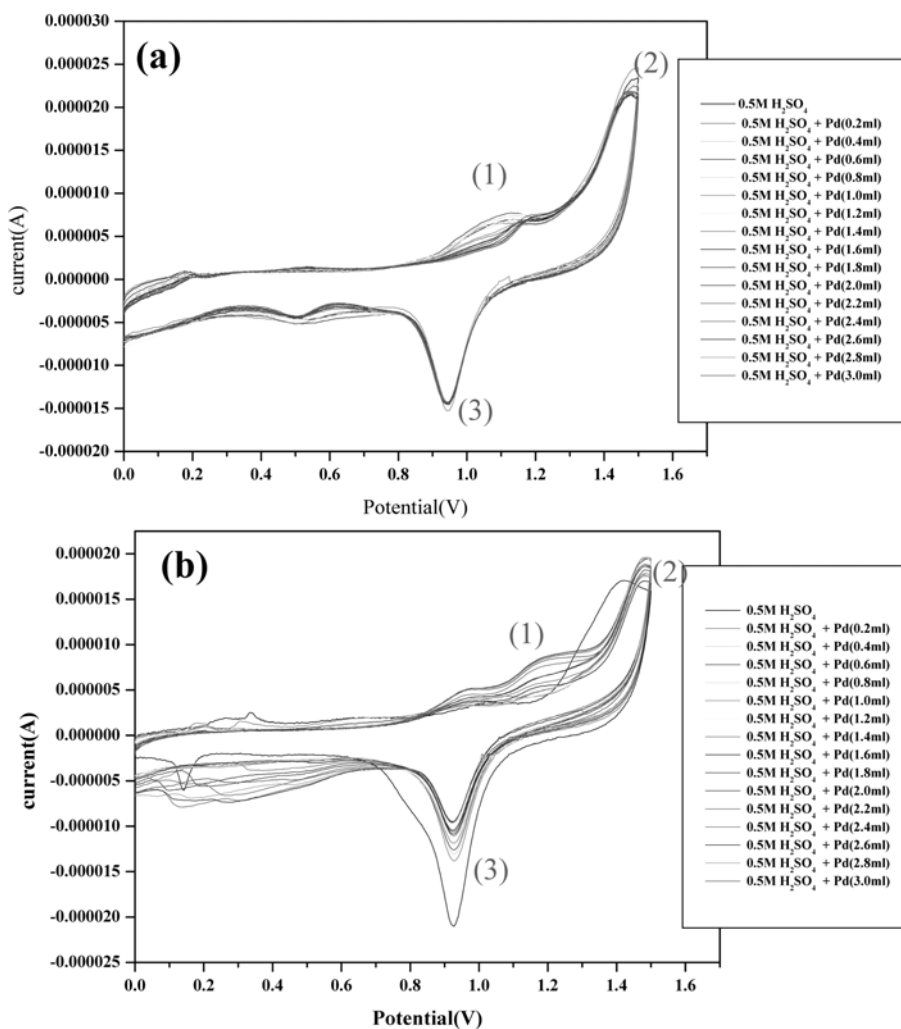


Fig. 8. CV curves of Au electrode in 0.5M H<sub>2</sub>SO<sub>4</sub> with Pd nanoparticles prepared by  $\gamma$ -irradiation (a) and prepared by e-beam (b).

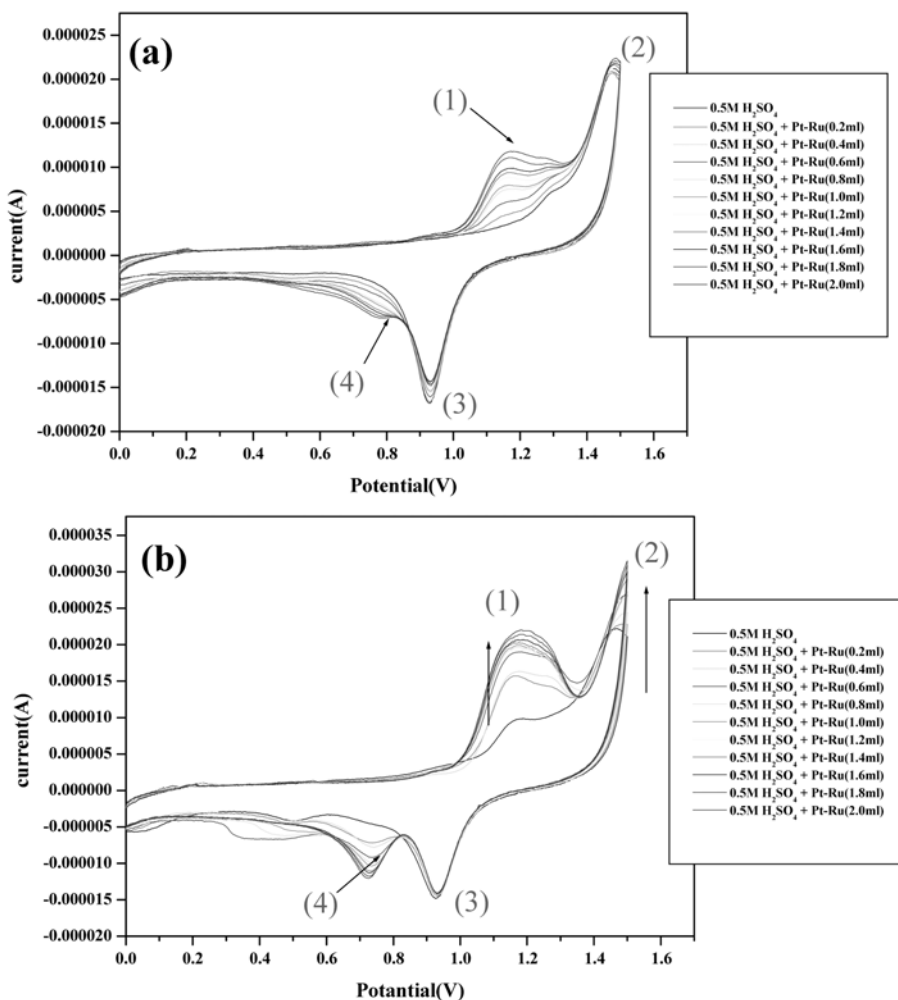


Fig. 9. CV curves of Au electrode in 0.5M H<sub>2</sub>SO<sub>4</sub> with Pt<sub>50</sub>-Ru<sub>50</sub> nanoparticles prepared by  $\gamma$ -irradiation (a) and prepared by e-beam (b).

Pd nanoparticles resulted two peaks around 0.9-1.2V. This interesting phenomenon clearly support that Pd nanoparticles with differential particle size were immobilized onto the Au electrode.

CV curves of Au electrode that show the immobilization of Pt<sub>50</sub>-Ru<sub>50</sub> nanoparticles prepared by  $\gamma$ -irradiation (a) and prepared by e-beam (b), are presented in Fig. 9. Peak (4) in Fig. 9(a) and Fig. 9(b) can be taken as representative of the immobilization of Pt<sub>50</sub>-Ru<sub>50</sub> nanoparticles into Au electrode surface. Clearly, there are subtle changes in the surface modification in these two cases. The differences in the size distributions between the nanoparticles colloids prepared

with  $\gamma$ -irradiation and EB manifest the differences in the surface modifications, as evident from the CVs (Fig. 9).

#### 4. Conclusions

PVP-protected Ag, Pd and Pt<sub>50</sub>-Ru<sub>50</sub> colloids were prepared without adding any specific reducing agent by  $\gamma$ -irradiation and electron beam at ambient temperature. The size of Ag, Pd, and Pt<sub>50</sub>-Ru<sub>50</sub> nanoparticles prepared electron beam irradiation were comparatively lesser than the respective nanoparticles prepared by  $\gamma$ -irradiation. The size distributions



were also different. These nanoparticles could be immobilized onto Au surface to result modified electrodes. These nanoparticles cover the Au surface to different extent depending on the distribution and size of the nanoparticles. The modified electrodes are expected to find applications as electro catalysts.

### Acknowledgement

This work was supported by the Science Foundation of Hannam University (2006).

### References

- Balan, L., Schneider, R., Billaud, D., Ghanbaja, J., *Mater. Lett.*, **59**, 1080-084 (2005).
- Gupta, A. K., Gupta, M., *Biomaterials*, **26**, 3995-4021 (2005).
- Xu, W., Xu, S., Ji, X., Song, B., Yuan, H., *Coll. Surf. B*, **40**, 169-172 (2005).
- Wang, H., Qiao, X., Chen, J., Ding, S., *Coll. Surf. A*, **256**, 21-25 (2005).
- Henglein, A., *J. Phys. Chem. B*, **104**, 2201-2203 (2000).
- Choi, S.-H., Lee, S.-H., Hwang, Y.-M., Lee, K.-P., Kang, H.-D., *Radiati. Phys. Chem.*, **67**, 517-521 (2003).
- Choi, S.-H., Zhang, Y.-P., Gopalan, A., Lee, K.-P., Kang, H.-D., *Coll. Surf. A*, **256**, 165-170 (2005).
- Li, T., Park, H. G., Lee, H.-S., Choi, S.-H., *Nano Tech.*, **15**, S660-S663 (2004).
- Andres, R.P., Averback, R.S., Brown, W.L., Brus, L.E., Goddard, W.A., Kaldor, A., Luoie, S.G., Moscovits, M., Peercy P.S., Riley, S.J., Siegel, R.W., Spaepen, F., Wang, Y., *J. Mater. Res.*, **43**, 704-736 (1989).
- Tolbert, S.H., Alivasatos, A.P., *Annu. Rev. Phys. Chem.*, **46**, 595-625 (1995).
- Horvath, J., Birringer, R., Gleiter, H., *Solid State Commun.*, **62**, 319-322 (1987).
- Qin, X.Y., Wu, B.M., Du, Y.L., Zhang, L.D., Tang, H.X., *Nanostruct. Mater.*, **7**, 383-391 (1996).
- Tanahashi, I., Yoshida, M., Manabe, Y., Tohda, T., *J. Mater. Res.*, **10**, 362-365 (1995).
- Gleiter, H., *Progress Mater. Sci.*, **33**(4), 223-315 (1989).
- Esumi, K., Wakabayashi, M., Torigoe, K., *Coll. Surf. A*, **109**, 55-62 (1996).
- Henglein, A., *Langmuir*, **15**, 6738-674 (1999).
- Yu, W., Liu, M., Liu, H., Zhen, J., *J. Colloid Inter. Sci.*, **210**, 218-221 (1999).
- Uemura, T.; Kitagawa, S., *J. Am. Chem. Soc.*, **125**, 7814-7815 (2003).
- De Cointet, C., Mostafavi, M., Khatouri, J., Keita, B., Nadjo, L., Belloni, J., *J. Phys. Chem. B*, **101**, 3512-3516 (1997).
- Suyal, G., *Thin Solid Films*, **426**, 53-61 (2003).
- Scholes, F.H., Furman, S.A., Lau, D., Rossouw, C.J., Davis, T.J., *J. Non-Crystalline Solids*, **347**(1-3), 93-99 (2004).
- Whelan, A.M., Brennan, M.E., Blau, W.J., Kelly, J.M., John M., *J. Nanosci. Nanotech.*, **4**(1/2), 66-68 (2004).
- Genzel, L., Martin, T.P., Kreibig, U.Z., *Phys. B*, **21**, 339-346 (1975).
- Malik, M. A., O'Brien, P., Revaprasadu, N., *J. Mater. Chem.*, **12**(1), 92-97 (2002).
- Zhou, Y., Itoh, H., Uemura, T., Naka, K., Chujo, Y., *Langmuir*, **18**(1), 277-283 (2002).
- Kapoor, S., *Langmuir*, **14**, 1021-1025 (1998).
- Guo, J.W., Zhao, T.S., Prabhuram, J., Wong, C.W., *Electrochim. Acta*, **50**, 1973-1983 (2005).
- Kuk, S.T., Wieckowski, A., *J. Power Sour.*, **141**, 1-7 (2005).
- Choi, J.-H., Park, K.-W., Park, I.-S., Nam, W.-H., Sung, Y.-E., *Electrochim. Acta*, **50**, 787-790 (2004).
- Sawyer, D.T., Roberts, Jr. J.L., *Experimental Electrochemistry for Chemists*, John Wiley & Sons, p. 67 (1974).
- Solla-Gullón, J., Rodes, A., Montile, V., Aldaz, A., Clavilier, J., *J. Electroanal. Chem.*, 554-555, 273-284 (2003).